ISSN 0036-0244, Russian Journal of Physical Chemistry A, 2016, Vol. 90, No. 6, pp. 1101–1114. © Pleiades Publishing, Ltd., 2016.
Original Russian Text © M.A. Shevchenko, M.I. Ivanov, V.V. Berezutski, V.S. Sudavtsova, 2016, published in Zhurnal Fizicheskoi Khimii, 2016, Vol. 90, No. 6, pp. 823–836.

CHEMICAL THERMODYNAMICS AND THERMOCHEMISTRY

Thermodynamic Properties of Alloys of the Binary In–La System[1]

M. A. Shevchenko, M. I. Ivanov, V. V. Berezutski, and V. S. Sudavtsova

Frantsevitch Institute for Problems of Materials Science, ul. Krzhizhanovskogo, 3, Kyiv 03142, Ukraine
e-mail: sud@ipms.kiev.ua, maximshevch@ukr.net

Received April 22, 2015

Abstract—The thermochemical properties of melts of the binary In–La system were studied by the calorimetry method at 1250–1480 K over the whole concentration interval. It was shown that significant negative heat effects of mixing are characteristic features for these melts. Using the ideal associated solution (IAS) model, the activities of components, Gibbs energies and the entropies of mixing in the alloys, and the phase diagram of this system were calculated. They agree with the data from literature.

Keywords: In–La binary system, thermodynamic properties of alloys.
DOI: 10.1134/S0036024416060248

Alloys of the rare-earth (Ln) metals with *p*-elements of the third group are promising as superconductors, catalysts and promoters, as well as cathode materials with various emission properties [1, 2]. However, there are quite few works in literature devoted to investigation of the alloys of indium with the lanthanides. Even when they have been conducted, it was only the alloys containing 75% indium or more that were studied. The reason for this is low availability of the components in pure state, as well as instability of their alloys in air. A complete thermodynamic analysis using CALPHAD method is only known for the systems In–La [2] and In–Eu(Yb) [3].

Nevertheless, in the rest, such alloys are quite simple objects for investigation. They are mostly low-melting, non-volatile, and do not interact with refractory metals (Mo, W) which can be used as crucible materials. This allows to fulfill the investigation of thermodynamic properties of the In–Ln liquid alloys using calorimetry method over a wide range of concentrations, which has already been done by us for the Eu–In [4] and Ce–In systems. The present work is devoted to study of thermochemical properties of the In–La system and modeling of other thermodynamic properties of these alloys. Investigation of a wide range of such systems, particularly Gd–In and In–Yb, will allow to establish the regularities of change of the interaction between the components in the In–Ln system series.

The In–La phase diagram was investigated by McMasters et al. [5] using thermal analysis, microscopy and X-ray diffraction methods. Seven intermetallics were found to exist: $LaIn_3$, $LaIn_2$, La_3In_5, $LaIn_x$, LaIn, La_2In, and La_3In. Three of them melt congruently ($LaIn_3$, La_3In_5, LaIn), other three undergo peritectic reactions ($LaIn_2$, La_2In, La_3In), and the last one ($LaIn_x$, which has approximate composition $La_{0.43}In_{0.57}$) exists in a narrow range of temperatures only (905°C < T < 1073°C), and there are only indirect proofs of its presence, i.e. the thermal effects. Two high-temperature modifications of lanthanum (β- and γ-La) form wide ranges of solid solutions, containing up to 3.5 and 10.2 at % In, respectively.

The solubility of La in liquid In (i.e., the liquidus curve of equilibrium of the $LaIn_3$ compound with the melt) was described in two works by different equations: $\log x_{La} = 0.88 - 2292/T$, 725 K < T < 975 K [6] and $\log x_{La} = -1.31 - 1100/T$, 500 K < T < 800 K [7]. These results are relatively similar at low temperatures; however, they diverge significantly at high temperatures. For example, at 800 K x_{La} = 1.04 mol % [6] and 0.21 mol % [7]; at 1000 K x_{La} = 3.87 mol % [6] and 0.39 mol % [7]. In the handbook [8] the results [6] are considered as more reliable, showing greater solubility of lanthanum in the liquid phase.

All these data on the phase equilibria in the In–La system are discussed in the reviews [9, 10] with comparison to the analogous In–Ln system. Similar information on the In–La phase diagram is given in the review [11] and the handbook [12].

Most investigations of the thermodynamic properties of the In–La alloys are dealing with the intermetallic $LaIn_3$ richest in indium. According to the results [6], at T = 975 K $\Delta_f H^0_{LaIn_3} = -53.65$ kJ/mol, $\Delta_f G^0_{LaIn_3} = -42.98$ kJ/mol, $\Delta_f S^0_{LaIn_3} = -10.95$ J/(mol K). The integral values ΔH, ΔS^{ex}, and ΔG^{ex} are calculated for the

[1] The article was translated by the authors.

homogeneous liquid alloys in the range $0 < x_{La} < 0.025$ from the activities of lanthanum measured using e.m.f. method. They show almost linear dependences on concentration in this range. Correspondingly, the partial values for lanthanum do not depend on concentration within $0 < x_{La} < 0.025$: $\Delta\overline{H}_{La} = -191.9$ kJ/mol, $\Delta\overline{S}^{ex}_{La} = -60.7$ J/(mol K), $\Delta\overline{G}^{ex}_{La} = -147.9$ (725 K) and -132.7 kJ/mol (975 K). Though the authors [6] relate all these values to the upper boundary of the temperature range of their investigation (975 K), it would be possibly more accurate to consider these enthalpies and entropies to be actual at the middle of the range, $(725 + 975)/2 = 850$ K.

A value $\Delta_f H^0_{LaIn_3} = -52.2$ kJ/mol was obtained [13] with dynamic differential calorimetry. Values $\Delta_f H^0_{LaIn_3} = -69.9$ and $\Delta_f H^0_{La_2In_3} = -61.1$ kJ/mol were determined [14] using calorimetry of dissolution in hydrochloric acid. Since the compound La_2In_3 ($x_{La} = 0.4$) has not been mentioned in other works, devoted to the In–La system, it was concluded in the review [9] that this results relates to the La_3In_5 ($x_{La} = 0.375$), which is the most refractory in this system.

Enthalpies of formation of solid In–La alloys at 23 different compositions were measured [15] using differential direct isoperibolic calorimetry. Unfortunately, the experiments of alloying La and In were done at very low temperature (250°C), so the reaction would complete only for the indium-rich ($x_{La} < 0.25$) alloys with the lowest melting temperature. At $x_{La} > 0.25$, a decrease of exothermic heat effects of formation of the alloys was observed, as well as significant scattering of experimental values. It should be noted that so strong shift of the minimum of the enthalpies of formation of the intermetallics towards indium is unlikely. It contradicts to the evaluations by the authors [16, 17], which predict not so highly asymmetric thermodynamic functions of mixing of the In–La alloys, due to small difference between the atomic radii of the components:

Compound	$LaIn_3$	$LaIn_2$	La_3In_5	LaIn	La_2In	LaIn
$-\Delta_f H$ [17], kJ/mol	−49	−62	−67	−71	−56	−43

Authors [15] determined that $\Delta_f H^0_{LaIn_3} = -58.7 \pm 4.2$ kJ/mol, and they suggest for equiatomic compositions $\Delta_f H^0_{LaIn}$ to be from −63 to −67 kJ/mol, though the measured $\Delta_f H$ do not exceed −60.7 kJ/mol in this field, due to incompleteness of the alloying reaction.

The In–La alloys were studied [18] using e.m.f. method at 1000 K. Unfortunately, the results contain many mistakes: the names of thermodynamic functions and their dimensions are mixed up in the tables. These mistakes were partly fixed in the handbook [8], and some numbers in the tables were corrected. Nevertheless, the obtained result remain doubtful. A value $\Delta_f H = -56.4$ kJ/mol is given for the $LaIn_3$ compound (per 4 atoms in the formula unit). However, much more exothermic $\Delta_f H$ are given for other four compounds, $LaIn_2$, LaIn, La_2In, and La_3In −76.7, −94.8, −124.4, and −97.1 kJ/mol, respectively [8]. In the initial work [18], these numbers are given in the column $\Delta\overline{H}_{In}$: −56.4, −76.7, −97.1, −110.9, −95.5 kJ/mol for the compositions $LaIn_3$, $LaIn_2$, LaIn, La_2In, La_3In, respectively. In any case, these values are almost twice more exothermic than the determined experimentally [14, 15] and estimated using the Miedema model [16, 17]. Besides, the authors [18] disconfirm the existence of the La_3In_5 compound, because they have not observed a step in the e.m.f. values at this composition.

According to the calculations by Bayanov [19], $\Delta_f H^0_{LaIn_3} = -117.15$ kJ/mol. This value is twice higher by absolute value than the majority of other literature data, so it cannot be considered reliable. Also, a value $\Delta_f H^0_{LaIn_3} = -53.7 \pm 2.6$ was determined using high-temperature direct synthesis calorimetry [20].

Thermodynamic properties of dilute solutions of La in liquid In were described [8] with an equation $\log\gamma_{La} = 3.097 - 9841/T$, hence $\Delta\overline{H}^{\infty}_{La} = -188.4$ kJ/mol, $\Delta\overline{S}^{\infty ex}_{La} = -59.3$ J/(mol K), $\Delta\overline{G}^{\infty ex}_{La} = -140.9$ kJ/mol at 800 K, −135.0 at 900 K, −129.1 at 1000 K.

Thermodynamic properties of the $LnIn_3$ intermetallics are described with common polynomial dependences from the atomic number of a lanthanide (excluding Eu, Yb), at two temperatures—298 and 775 K [21]. There is a decrease of exothermic effects of $LnIn_3$ formation from −(58–55) kJ/mol for light lanthanides to −35 kJ/mol for Lu. However, the most exothermic values of $\Delta_f H^0_{LnIn_3}$ are observed not for lanthanum, but for cerium, praseodymium, and neodymium. According to these dependences, the $LaIn_3$ has $\Delta_f H_{298} = -55.0$ kJ/mol, $\Delta_f H_{775} = -55.1$ kJ/mol, which correlates with the data [13–18, 20].

So, there are no experimental data in the literature on the thermochemical properties of the In–La melts over the whole concentration range, and of the intermetallics rich in lanthanum, and they are of significant interest. The scope of the present work is to investigate the enthalpies of mixing of melts in the In–La system using calorimetry, and to create a thermodynamic model to describe our and literature data, including the phase diagram.

Table 1. Experimental values of partial and integral mixing enthalpies of the In–La melts (kJ/mol)

x_{La}	$-\Delta\overline{H}_{In}$	$-\Delta H$	x_{La}	$-\Delta\overline{H}_{In}$	$-\Delta H$	x_{La}	$-\Delta\overline{H}_{La}$	$-\Delta H$
	Series 1 1460 K			Series 2 1250 K			Series 3 1370 K	
0.9914	122.6	1.06	0.9886	136.9	1.56	0.0067	156.8	1.04
0.9828	120.7	2.10	0.9773	141.2	3.16	0.0132	154.5	2.06
0.9743	115.9	3.08	0.9658	134.0	4.70	0.0200	152.3	3.09
0.9657	121.3	4.12	0.9544	138.1	6.27	0.0268	156.8	4.15
0.9574	118.9	5.11	0.9430	135.7	7.81	0.0341	154.0	5.27
0.9490	117.2	6.10	0.9318	135.8	9.34	0.0415	146.1	6.35
0.9406	114.3	7.04	0.9207	132.1	10.79	0.0499	145.5	7.58
0.9324	117.2	8.01	0.9099	137.1	12.28	0.0584	149.8	8.85
0.9233	114.9	9.05	0.8993	137.8	13.74	0.0670	147.9	10.11
0.9142	115.5	10.10	0.8884	130.3	15.15	0.0758	151.6	11.45
0.9052	110.4	11.09	0.8777	126.2	16.49		1400 K	
0.8963	113.2	12.09	0.8672	135.3	17.92	0.0810	144.1	12.21
0.8875	109.7	13.05	0.8566	120.5	19.17	0.0893	152.0	13.47
0.8789	110.9	14.00	0.8460	135.8	20.61	0.0977	140.1	14.64
0.8704	107.8	14.91	0.8354	128.4	21.96	0.1065	152.1	15.97
0.8621	111.1	15.83	0.8250	119.7	23.18	0.1155	135.8	17.18
0.8538	104.6	16.68		1270 K		0.1253	140.3	18.55
0.8456	97.2	17.46	0.8147	116.8	24.35	0.1351	147.0	19.98
0.8375	107.3	18.31	0.8044	119.1	25.54	0.1447	147.4	21.40
0.8296	106.6	19.15	0.7945	124.3	26.77	0.1546	134.2	22.71
0.8217	97.6	19.90	0.7847	119.1	27.90	0.1644	139.9	24.06
	1430 K			1480 K		0.1739	131.6	25.29
0.8138	98.2	20.65	0.7756	95.6	24.43*		1420 K	
0.8060	102.4	21.43	0.7664	94.0	25.26	0.1737	137.9	25.26
0.7982	107.1	22.25	0.7574	95.8	26.09	0.1815	131.0	26.25
0.7906	111.2	23.1	0.7484	92.7	26.87	0.1874	130.2	27.00
0.7831	105.8	23.89	0.7396	92.4	27.64	0.1948	129.2	27.94
0.7758	98.6	24.59	0.7310	91.9	28.40	0.2024	121.4	28.81
0.7686	97.4	25.27	0.7225	92.7	29.15	0.2090	119.7	29.57
0.7614	100.6	25.97	0.7141	85.6	29.79	0.2150	124.7	30.30
0.7543	101.3	26.67	0.7060	86.6	30.44	0.2208	121.3	30.97
0.7472	100.8	27.37	0.6978	87.6	31.11	0.2269	119.7	31.66
			0.6897	87.2	31.76	0.2329	125.2	32.38
			0.6817	88.1	32.41	0.2390	120.2	33.08
			0.6739	86.9	33.03	0.2453	111.6	33.73
			0.6662	81.6	33.59	0.2515	110.0	34.36
			0.6587	85.4	34.17	0.2523	110.0	34.44
			0.6512	82.7	34.72	0.2595	112.5	35.19
			0.6438	75.8	35.19	0.2658	110.6	35.83
			0.6366	74.7	35.63	0.2721	107.5	36.45

Table 1. (Contd.)

x_{La}	$-\Delta\overline{H}_{In}$	$-\Delta H$	x_{La}	$-\Delta\overline{H}_{In}$	$-\Delta H$	x_{La}	$-\Delta\overline{H}_{La}$	$-\Delta H$
			0.6295	76.3	36.09	0.2787	103.2	37.05
			0.6222	74.9	36.53	0.2858	102.0	37.69
			0.6151	73.3	36.96	0.2928	95.5	38.26
			0.6080	77.3	37.42	0.2997	94.5	38.81
			0.6011	74.7	37.85	0.3068	94.5	39.38
			0.5943	69.4	38.20	0.3138	90.6	39.89
			0.5881	77.8	38.61	0.3209	86.4	40.37
			0.5821	77.3	39.01	0.3249	75.8	40.58
			0.5757	77.7	39.44	0.3288	91.9	40.88
			0.5694	75.8	39.83	0.3328	79.4	41.11
			0.5632	70.7	40.17	0.3368	62.9	41.24
			0.5571	69.8	40.49	0.3416	67.0	41.42
			0.5512	69.8	40.80	0.3462	71.7	41.64
			0.5454	64.8	41.05	0.3516	59.2	41.78
			0.5397	64.0	41.29	0.3568	58.5	41.92
			0.5341	60.4	41.49	0.3619	52.2	42.00
			0.5284	66.4	41.75	0.3669	52.2	42.08
			0.5229	64.4	41.99	0.3721	50.1	42.14
			0.5174	62.6	42.21	0.3771	50.1	42.21
			0.5119	58.3	42.38	0.3823	39.6	42.19
			0.5064	60.2	42.57	0.3876	45.4	42.21
			0.5010	57.6	42.73	0.3927	43.5	42.22
			0.4957	54.5	42.86	0.3978	40.8	42.21
			0.4902	56.3	43.01	0.4029	39.1	42.19
			0.4847	56.2	43.15	0.4079	36.3	42.14
			0.4794	52.0	43.25	0.4128	34.7	42.08
			0.4742	51.9	43.34	0.4178	31.3	41.98
			0.4689	50.8	43.42	0.4227	24.2	41.84
			0.4637	49.3	43.49	0.4275	25.2	41.70
			0.4586	47.3	43.53	0.4325	22.2	41.53
			0.4536	49.8	43.60	0.4374	29.9	41.43
			0.4486	49.4	43.66			
			0.4436	48.8	43.72			
			0.4388	47.5	43.76			
			0.4339	45.4	43.78			
			0.4292	45.6	43.80			
			0.4243	45.4	43.82			
			0.4195	42.5	43.80			
			0.4147	42.6	43.79			
			0.4100	41.9	43.77			

* A recalculation of ΔH was made due to significant change in temperature, assuming that $\Delta\overline{H}_{In}^{1480} \approx \Delta\overline{H}_{In}^{1250-1270} + 20$ kJ/mol in the range $0.78 < x_{La} < 1$. The adjusting coefficient (20 kJ/mol) is taken from comparison of the results of the series 1 and 2.

EXPERIMENTAL PART

A detailed description of experimental technique is given in [22]. The experiments were conducted in molybdenum crucibles over the whole concentration range. Owing to the temperatures chosen as low as possible to keep away from formation of the In–La intermetallics, we managed to avoid the vaporization of the components, and the interaction of alloys with the crucible material.

Two series of experiments were conducted from the lanthanum side, and one from the indium side (Table 1). Starting masses of pure metals in the crucible were 1.6–1.8 g; the samples of mass 0.014–0.044 g were dropped into the crucible. The calorimeter was calibrated at the beginning of the experimental series with the samples of the same metal as was in the crucible. The enthalpy change between the solid metal at room temperature (298 K) and the liquid at the experimental temperature was calculated accordingly to [23]. Then, the calibration was periodically repeated (alternating 3–4 samples for calibration with 10–20 major samples of the second component). Either molybdenum or the same first component was used for that, since the partial enthalpies of the latter are small values and may be calculated using the Gibbs-Duhem equation. These repeated calibrations allowed us to control the change of the heat exchange coefficient of the calorimeter (i.e., its apparent heat capacity), which increased smoothly 1.2–1.4 times during the whole series, due to increasing mass of the alloy in the crucible.

The partial enthalpies of mixing of the components ($\Delta\overline{H}_i$) were calculated using the equation

$$\Delta\overline{H}_i = -\Delta H_{298}^{T_0}(i) + \frac{k}{n_i}\int_{\tau_0}^{\tau_\infty}(T - T_0)\,dt,$$

where k is the heat exchange coefficient of the calorimeter, determined using calibration component A as:

$$k = \Delta H_{298}^{T_0}(\mathrm{A})\,n_\mathrm{A}\Big/\int_{\tau_0}^{\tau_\infty}(T - T_0)\,dt;$$

$\Delta H_{298}^{T_0}(i)$ is the enthalpy change between the solid metal i at 298 K and the liquid at the temperature of the experiment, from [23]; n_i is the molar quantity of metal in the sample; $\int_{\tau_0}^{\tau_\infty}(T - T_0)\,dt$ is the area under the peak on a thermal curve (τ_0, τ_∞ are the start and the end times of the heat effect recording, respectively, T is the temperature, T_0 is the equilibrium temperature, t is time).

Integral mixing enthalpies of the melt were calculated through the equation

Table 2. Partial and integral mixing enthalpies of the In–La melts at 1450 K, kJ/mol

x_La	$-\Delta H$	$-\Delta\overline{H}_\mathrm{In}$	$-\Delta\overline{H}_\mathrm{La}$
0	0	0	153.6 ± 6.4
0.1	15.1 ± 0.7	0.3 ± 0.0	148.2 ± 6.2
0.2	29.2 ± 1.4	4.0 ± 0.2	130.1 ± 5.4
0.3	39.3 ± 1.9	18.4 ± 0.8	88.0 ± 3.7
0.4	43.4 ± 2.1	36.6 ± 1.6	53.6 ± 2.2
0.5	43.0 ± 2.0	54.5 ± 2.4	31.4 ± 1.3
0.6	38.9 ± 1.8	72.3 ± 3.2	16.7 ± 0.7
0.7	32.0 ± 1.5	89.3 ± 4.0	7.4 ± 0.3
0.8	22.7 ± 1.1	104.1 ± 4.6	2.4 ± 0.1
0.9	11.8 ± 0.6	114.7 ± 5.1	0.4 ± 0.0
1	0	121.7 ± 5.4	0

$$\Delta H^{n+1} = \Delta H^n + \left(\Delta\overline{H}_i^{n+1} - \Delta H^n\right) \times \left(x_i^{n+1} - x_i^n\right)\Big/\left(1 - x_i^n\right),$$

which is valid when the change of concentration of the ith component from x_i^n to x_i^{n+1} is small at addition of the $(n+1)$th sample.

The obtained experimental points were approximated with smooth concentration dependences accordingly to the ideal associated solution (IAS) model, which is described below in detail. Partial and integral mixing enthalpies of melts of the In–La system at 1250–1480 K are presented in Fig. 1, and their values at rounded concentrations with errors (smoothed using IAS model, at 1450 K)—in Table 2. The errors were evaluated as the mean square deviations of the experimental points from the smooth curves. Each function ΔH, $\Delta\overline{H}_\mathrm{La}$, $\Delta\overline{H}_\mathrm{In}$ was assumed to have errors proportional to its absolute value.

Since the calculation of the thermodynamic properties using IAS model requires special software and is not always available, it is desirable to provide a simpler description of the concentration dependences of the thermodynamic properties. However, such expression is less accurate to describe the experimental data, and it is valid over a limited temperature range only, $T = 1450 \pm 100$ K. The obtained set of the partial and integral enthalpies of mixing was approximated with polynomial dependences (kJ/mol):

$$\Delta\overline{H}_\mathrm{La} = (1 - x_\mathrm{La})^2(-153.6 - 459.6x_\mathrm{La} + 1498.5x_\mathrm{La}^2 - 951.4x_\mathrm{La}^3),$$

$$\Delta\overline{H}_\mathrm{In} = x_\mathrm{La}^2(76.2 - 1458.6x_\mathrm{La} + 2212.1x_\mathrm{La}^2 - 951.4x_\mathrm{La}^3),$$

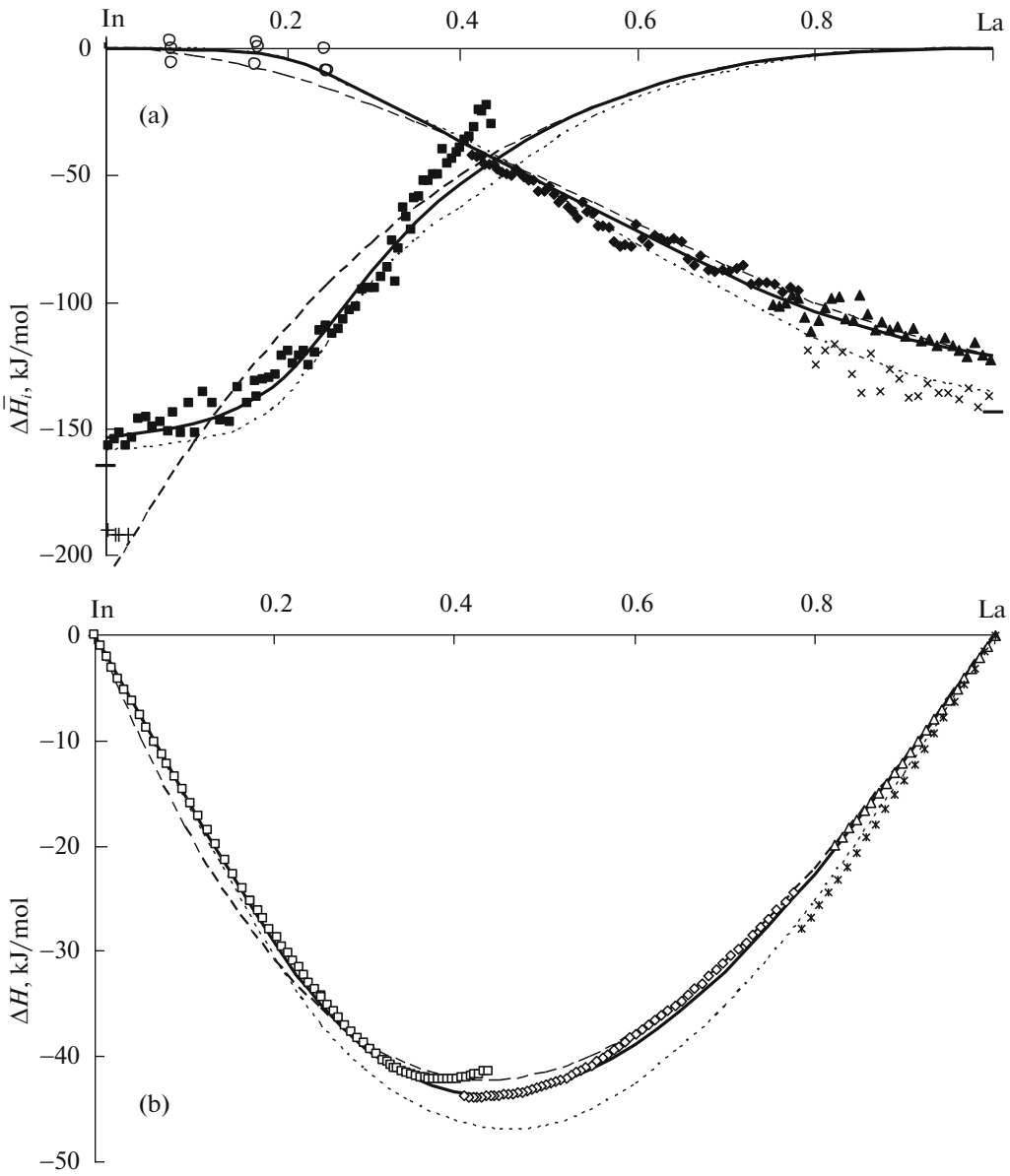

Fig. 1. Partial (a) and integral (b) enthalpies of mixing of the In–La melts, investigated by us experimentally (series 1: ▲ $\Delta\overline{H}_{In}$, △ ΔH—1430–1460 K; series 2: × $\Delta\overline{H}_{In}$, * ΔH—1250–1270 K; ◆ $\Delta\overline{H}_{In}$, ◇ ΔH—1480 K; series 3: ■ $\Delta\overline{H}_{La}$, □ ΔH, ○ $\Delta\overline{H}_{In}$—1370–1420 K) and approximated using IAS model (—— 1450 K, - - - - - - 1200 K); data from literature (– – assessment [2]; $-\Delta\overline{H}^{\infty}_{In,La}$, Miedema model [17], not depending on temperature; + $\Delta\overline{H}_{La}$ [6], 625–975 K, e.m.f. method).

$$\Delta H = x_{La}(1-x_{La})(-153.6 - 229.8x_{La} + 499.5x_{La}^2 - 237.8x_{La}^3).$$

Integral excess entropies (J/(mol K)), evaluated from the IAS model (see below), were approximated with the dependence:

$$\Delta S^{ex} = x_{La}(1-x_{La})(-53.4 - 115.5x_{La} + 213.5x_{La}^2 - 92.7x_{La}^3).$$

DISCUSSION OF THE RESULTS

The obtained data, together with those from literature, were treated by means of the software complex developed by us, based on the model of ideal associated solutions (IAS). The same method has been used before to treat the results of calorimetrical investigation of liquid alloys simultaneously with the literature data from phase equilibria and thermodynamic properties of many metallic systems with strong interaction between the components [24–26]. The correctness of this method has been shown in the work [27]. Appar-

ently, this model is only unsuitable for description of thermodynamic properties of liquid metallic alloys with positive enthalpies of mixing.

All available experimental data, supplemented by a list of compounds in the solid alloys (accordingly to the phase diagram) and assumed associates in the liquid alloys, were inserted into the created program. Arbitrary starting values of enthalpies ($\Delta_f H^{sol}$, $\Delta_f H^{liq}$) and entropies ($\Delta_f S^{sol}$, $\Delta_f S^{liq}$) of formation were set for these compounds in the solid alloys and the associates; then they served as variable parameters during the optimization. In the case of correct list of the associates and non-contradictory literature data, some combination of values of these parameters gives satisfactory agreement with all those experimental data for the alloys.

The equilibrium concentrations of the associates in the melt at given composition and temperature correspond to a minimum of the function

$$\Delta G = RT\left(a_A \ln a_A + a_B \ln a_B + \sum_{n=1}^{N} x_n\left(\frac{\Delta G_n}{RT} + \ln x_n\right)\right)\Bigg/\left(1 + \sum_{n=1}^{N}(i_n + j_n - 1)x_n\right),$$

where $\Delta G_n = \Delta_f H_n^{liq} - T\Delta_f S_n^{liq}$; $a_A = x_{A_1}$ and $a_B = x_{B_1}$ are the molar fractions of the monomers, which are similar to the activities of the components due to IAS model principles; x_n are the molar fractions of the associates. The normalizing conditions are

$$a_A + a_B + \sum_{n=1}^{N} x_n = 1,$$

$$1 - x_A = x_B = \left(a_B + \sum_{n=1}^{N} x_n j_n\right)\Bigg/\left(a_A + a_B + \sum_{n=1}^{N} x_n(i_n + j_n)\right),$$

where x_A, x_B are the total molar fractions of the components in the melt.

As soon as the minimum of ΔG and the corresponding values of a_A, a_B, and x_n ($n = 1, \ldots, N$) are found, we can calculate other thermodynamic functions, for example

$$\Delta H = \left(\sum_{n=1}^{N} \Delta_f H_n \cdot x_n\right)\Bigg/\left(1 + \sum_{n=1}^{N}(i_n + j_n - 1)x_n\right).$$

We used self-created programs to calculate the thermodynamic properties from the given $\Delta_f H_n^{liq}$ and $\Delta_f S_n^{liq}$ parameters, as well as to optimize these parameters in order to achieve the best approximation of the thermodynamic properties to the experimental data.

To describe the thermodynamic properties of the In–La system, we chose a model accounting for formation of 5 associates: $LaIn_3$, $LaIn_2$, LaIn, La_2In, La_3In. All of them have rather simple composition (no more than 4 atoms), and correspond to the compounds existing in the solid alloys.

Problems arose while modeling the liquidus curve of the phase diagram in the field of equilibrium of the LaIn compound with the melt. According to the literature data [5], there is asymmetric liquidus in this field—steep at $x_{La} < 0.5$ and flat at $x_{La} > 0.5$. The authors of successive reviews [9, 10, 12] did not spend attention on this peculiarity, and it was only at first application of the CALPHAD method [2] that revealed impossibility to describe this field within a model using smooth dependences of thermodynamic functions on the melt concentration. We also faced the same problem at modeling the thermodynamic properties of the In–La alloys.

Moreover, none of the reviews of the indium-lanthanide phase diagrams discusses why the LaIn compound is considered stoichiometric, without any homogeneity ranges in solid state. Actually, almost all other analogous LnIn compounds are shifted in composition towards the lanthanide ($x_{Ln} \approx 0.52$) and/or have a solid solution range up to 5 at %. The data on the crystal structure of the LaIn compound are ambiguous, too. So, we set the composition $La_{13}In_{12}$ when modeling this compound, which significantly facilitated obtaining a consistent thermodynamic model, and agrees with the construction of the In–Pr(Nd, Sm, Gd, Tb, Dy, Ho, Yb) systems. However, we need to note that this assumption requires experimental confirmation. In particular, the existence homogeneity range and its size for this compound should be tested, while now we neglect it.

The $LaIn_x$ compound (of approximate composition $La_{0.43}In_{0.57}$) neither has a field of equilibrium with the melt, nor exists at low temperatures. The only facts indicating its presence are thermal effects at 905 and 1073°C, which are identified in [5] as low and high boundaries of stability of the compound $LaIn_x$. This feature was never observed for any other In–Ln systems. Thus, the existence of the $LaIn_x$ compound is doubtful. We exclude it from our model, since it does affect the liquidus shape.

The obtained parameters of the IAS model for the In–La system are presented in Table 3.

Most solid phases were treated as stoichiometric, and only for the γ-La phase homogeneity ranges were described by introducing the concentration dependences of the Gibbs energies of formation (kJ/mol, $x \equiv x_{La}$):

$$G_{(\gamma\text{-La})} = (1-x)G_{In}^T + xG_{La}^T + RT(x\ln x + (1-x)\ln(1-x)) + (-134 + 0.0524T)(1-x) + 20.3(1-x)^2.$$

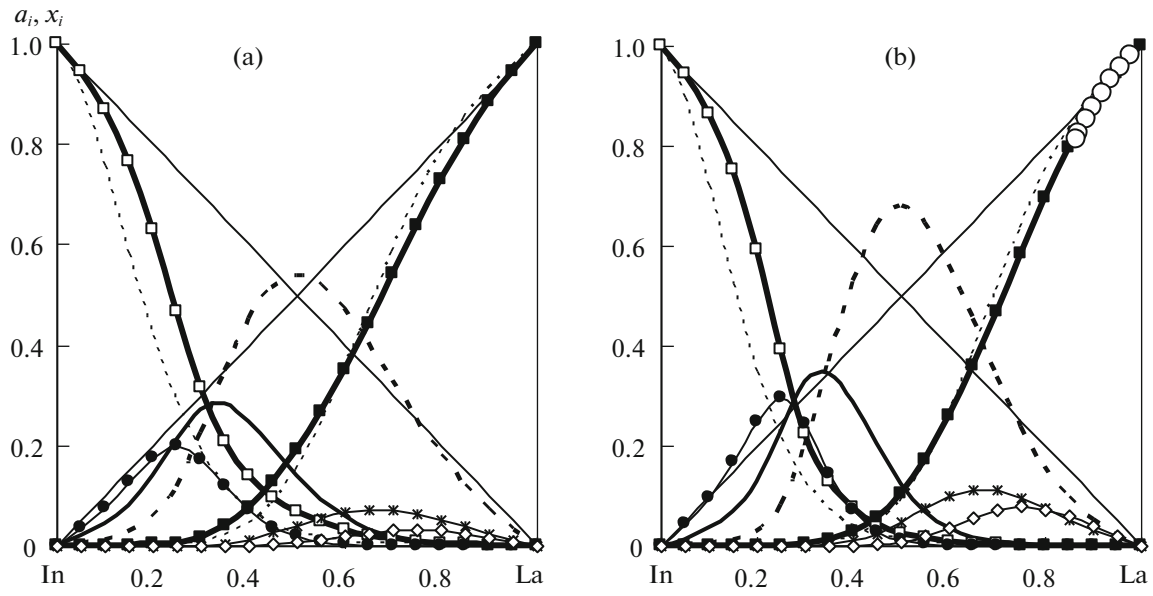

Fig. 2. Activities of the pure components (a_i: —□— In, —■— La) and molar fractions of the associates (x_i: —◆— $LaIn_3$, —— $LaIn_2$, - - - LaIn, —✱— La_2In, —◇— La_3In) in the In–La melts (including undercooled) at 1450 K (a) and 1200 K (b), according to the obtained IAS model. Data from literature: ○—activities of La at 1194 K [5], calculated from liquidus temperatures of the phase diagram; - - - —a_i, assessment [2].

Though, according to [10, 12], β-La also gives a wide range of solid solutions, we did not accounted for that, because: (1) this field is not in equilibrium with the melt, which properties are the primary objective of this study; (2) there are no exact data in the literature on the concentration boundaries of the solid solutions. All formation enthalpies and entropies of associates and intermetallics were assumed independent on temperature.

It is clear from Fig. 1 that the IAS model describes the experimental values of partial and integral enthalpies of mixing well, including their temperature dependences. Our results are also very close to the assessment [2]; their main difference is lower steepness of $\Delta\overline{H}_{La}$ in the range $0 < x_{La} < 0.25$.

Table 3. Enthalpies (kJ/mol) and entropies (J/(mol K)) of formation of the associates (liq) and intermetallics (sol) in the In–La system at 298 K

Composition	x_{La}	$-\Delta_f H^{liq}$	$-\Delta_f S^{liq}$	$-\Delta_f H^{sol}$	$-\Delta_f S^{sol}$
$LaIn_3$	0.25	41.8	16.7	52.3	16.7
$LaIn_2$	0.333	46.3	17.7	54.0	15.7
La_3In_5	0.375			53.8	14.9
LaIn	0.5	51.8	20.2		
$La_{13}In_{12}$	0.52			51.2	14.4
La_2In	0.667	45.2	23.3	41.7	12.4
La_3In	0.75	42.3	23.8	36.2	13.1

The calculated activities of the components (Fig. 2) show significant negative deviations from the Raoult's law, which become stronger at lower temperatures. The same as for the enthalpies of mixing, they have slightly asymmetric shape, as the minima of ΔH and ΔG are shifted towards indium. According to the IAS model, the greatest concentrations in the melts are inherent for the simplest associate LaIn.

From the IAS model, the temperature dependences of the partial enthalpies, Gibbs energies and entropies of the components of the In–La system at infinite dilution (Fig. 3) all have slow tendency to ideality at high temperatures. This is in agreement with the general regularities [28]. Modeled $\Delta\overline{S}^{\infty ex}_{La}$ agree with the data [6, 8], but $\Delta\overline{H}^{\infty}_{La}$ and $\Delta\overline{G}^{\infty ex}_{La}$ are significantly smaller in absolute value than the literature data.

The Gibbs energies of mixing of the In–La melts have less negative values, and the entropies of mixing have more negative values than estimated in [2] (Figs. 4, 5). Activities of lanthanum (Fig. 2b) and its partial excess Gibbs energies (Fig. 4) agree better with the experiment (more exactly, with the calculation from the experimental liquidus temperatures) [5],

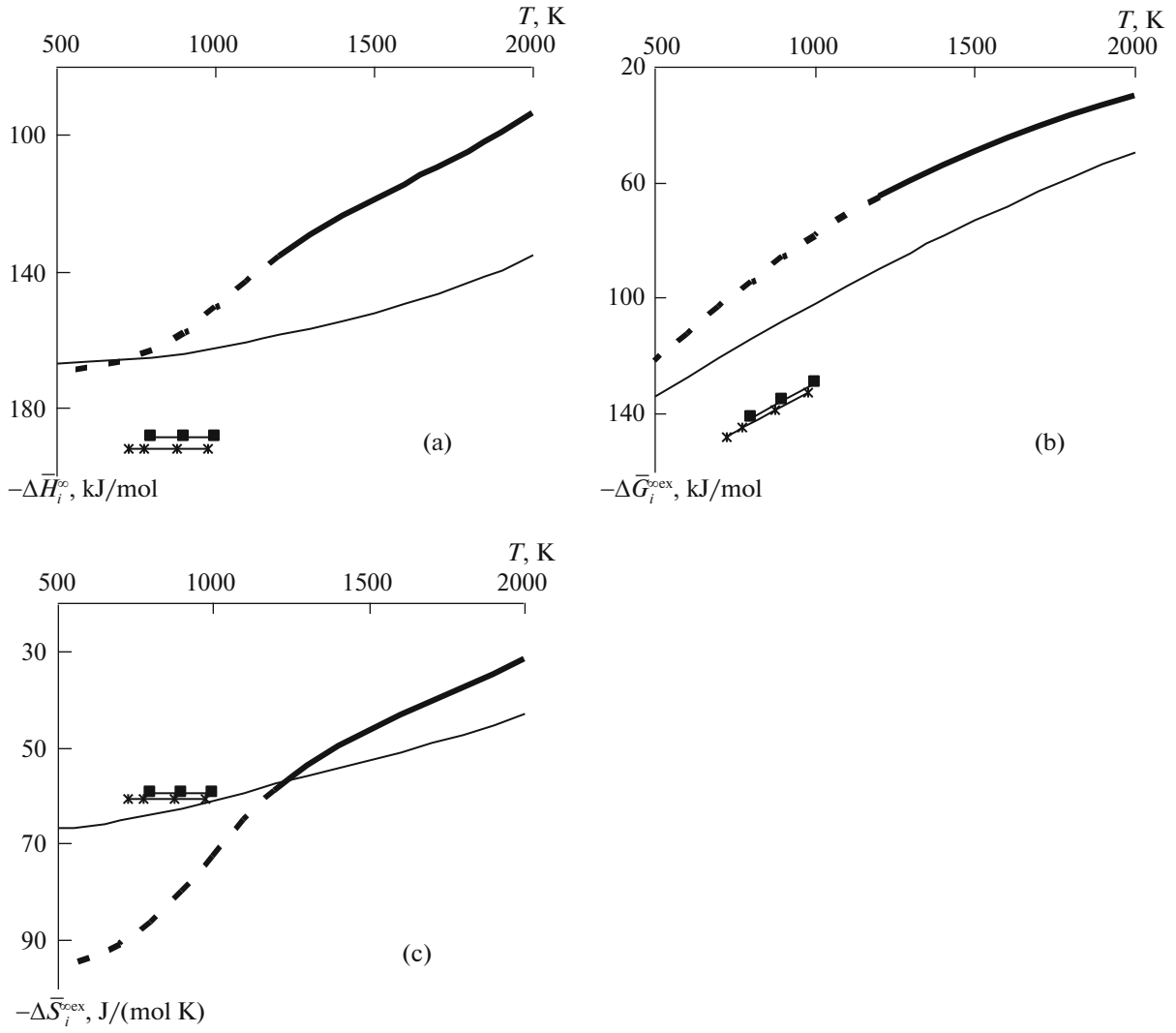

Fig. 3. Temperature dependences of the partial enthalpies (a) excess Gibbs energies, (b) and excess entropies, (c) of the components of the In–La melts at infinite dilution (▬▬ In in La, ——— La in In, ▪ ▪ ▪ In in undercooled La), according to the IAS model, and the data from literature [8] (■—■—■) and [6] (✱—✱—✱) (La in In).

than the estimation [2], though all these values are quite close to each other.

The enthalpies and Gibbs energies of formation of the $LaIn_3$ intermetallic, calculated by us (Figs. 6, 7), agree with the least exothermic data throughout the literature [13–18], as well as with the Miedema model [17]. The model [17] gives for liquid alloys $\Delta\overline{H}_{La}^{\infty} = -165$, $\Delta\overline{H}_{In}^{\infty} = -144$ kJ/mol. This agrees well with the values we obtained experimentally and optimized using the IAS model ($\Delta\overline{H}_{La}^{\infty} = -159.0$; $\Delta\overline{H}_{In}^{\infty} = -136.1$ kJ/mol at 1200 K). This also correctly reflects the slightly asymmetric shape of the concentration dependence of ΔH, the minimum of it shifted towards indium (the component with smaller atomic volume).

The calculated liquidus and solidus curves/polylines of the phase diagram (Fig. 8, Table 4) agree well with the literature [2, 5, 6] in the most part of the concentration range. The liquidus for the indium-rich alloys (Fig. 9) also reproduces well the data [6, 7]—at least within the difference between the results of those two works. However, for adequate description of the equilibrium of LaIn with the melt, it was necessary to change its stoichiometry to $La_{13}In_{12}$ ($x_{La} = 0.52$). Moreover, instead of peritectic decomposition reaction of La_2In to LaIn (more exactly, $La_{13}In_{12}$) and the liquid at heating, it was necessary to assume congruent melting of La_2In and the eutectic between $La_{13}In_{12}$ and La_2In. The temperatures of these two newly assumed invariant reaction are very close to each other, and

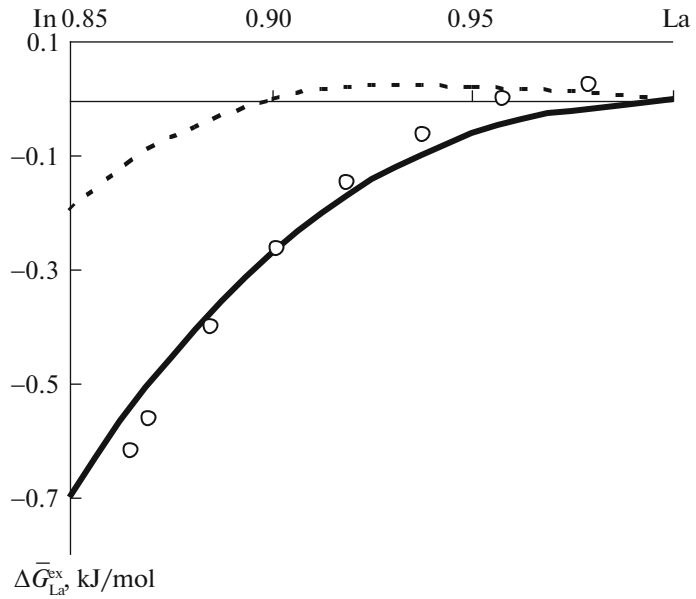

Fig. 4. Partial excess Gibbs energies of lanthanum in the In–La melts, rich in La: data [5], calculated for 1194 K from experimental liquidus points of the phase diagram (○); CALPHAD assessment [2] (- - -), 1200 K; our calculation using the IAS model (——), 1200 K.

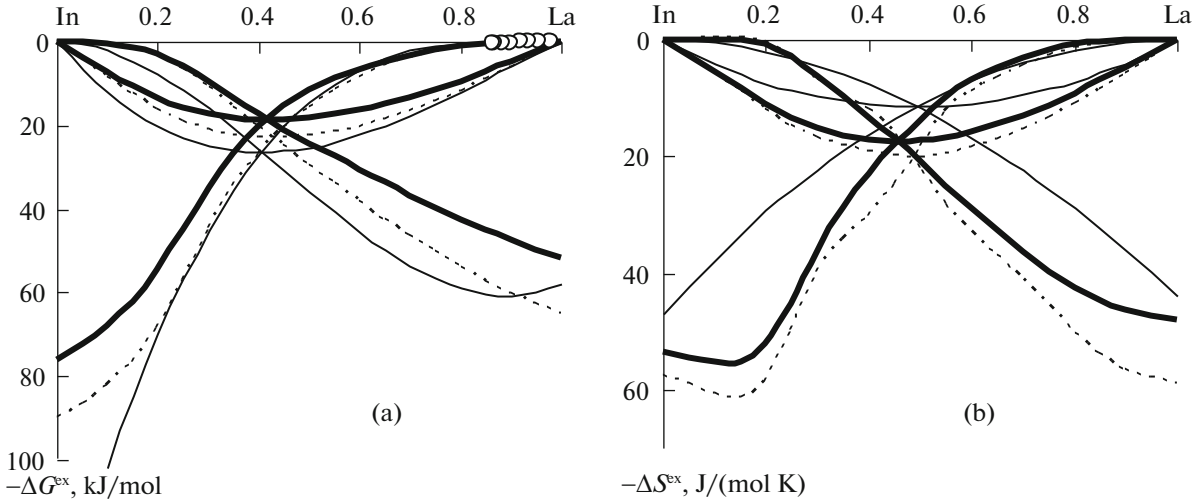

Fig. 5. Partial and integral excess Gibbs energies (a) and entropies (b) of mixing of the In–La melts, calculated using the IAS model at 1200 (- - - - -) and 1450 K (——); assessment [2] (——), 1450 K; and calculated $-\Delta G^{ex}_{La}$ [5] (○) from the experimental liquidus points of the phase diagram, 1194 K.

correspond to the temperature of the old peritectic Liq + LaIn = La_2In [5].

To sum up, the enthalpies of mixing of the In–La liquid alloys are great exothermic values in the whole concentration range. The activities of the components, Gibbs energies and entropies of mixing of the alloys in this system, and its phase diagram, all calculated using IAS model, agree with most literature data. The optimized thermodynamic model of the In–La alloys in the wide range of concentration and temperature mostly confirms the results of the previous modeling [2]; however, its

Table 4. Invariant liquidus points of the In–La phase diagram

Reaction	x_{La}^{liq}, at %	$x_{La}^{sol_1}$, at %	$x_{La}^{sol_2}$, at %	T, K	Reaction type
$Liq = In + LaIn_3$	0.5	0	25	428	Eutectic
	0.4	″	″	427.4	
	<0.1	″	″	429.8	
$Liq = LaIn_3$	25	25		1413	Congruent
	″	″		1409	
	″	″		1405.3	
$Liq = LaIn_3 + LaIn_2$	28.8	25	33.3	1393	Eutectic
	28.42	″	″	1397	
	28.3	″	″	1393	
$Liq + La_3In_5 = LaIn_2$	32	33.3	37.5	1426	Peritectic
	32.43	″	″	1424	
	32.2	″	″	1426	
$Liq = La_3In_5$	37.5	37.5		1458	Congruent
	″	″		1454	
	″	″		1463.7	
$Liq = La_3In_5 + LaIn$	46	37.5	50	1359	Eutectic
	46.4	″	″	1376	
$Liq = La_3In_5 + La_{13}In_{12}$	47.1	″	52	1372.5	
$Liq = LaIn$	50	50		1398	Congruent
	″	″		1387	
$Liq = La_{13}In_{12}$	52	52		1395	
$Liq + LaIn = La_2In$	70.4	50	66.7	1228	Peritectic
	66.84	″	″	1211	Peritectic
$Liq = La_{13}In_{12} + La_2In$	65.3	52	″	1230	Eutectic
$Liq = La_2In$ (IAS model)	66.7	66.7		1232	Congruent
$Liq + La_2In = La_3In$	80.9	66.7	75	1089	Peritectic
	79.55	″	″	1087	
	78.7	″	″	1087.5	
$Liq = La_3In + \gamma La(BCC)$	86.5	75	89.8	1015	Eutectic
	85.63	″	≈92	1019	
	85.3	″	89.9	1013	

The first row in each cell is from [5], the second is from [2], and the third is the present IAS model; IAS model for Liq = La2In.

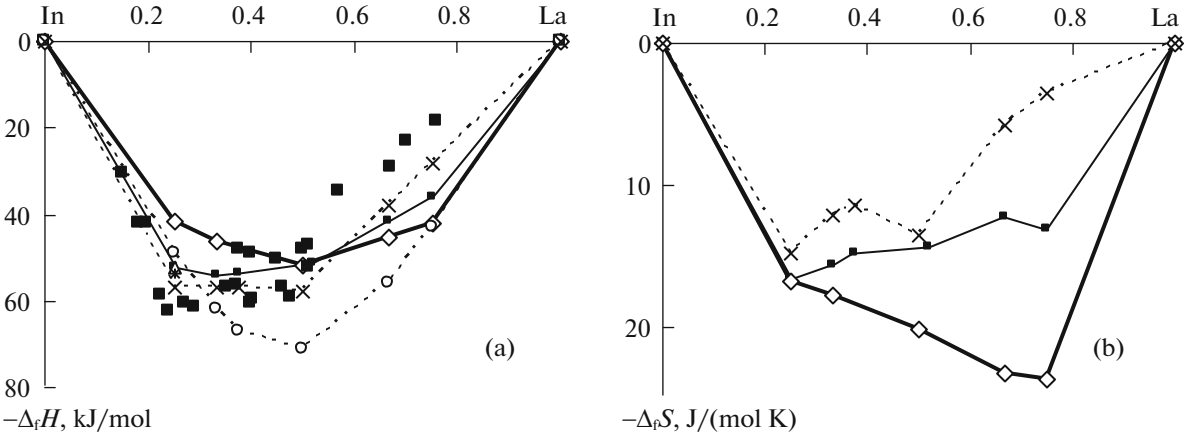

Fig. 6. Enthalpies (a) and entropies (b) of formation of the associates in the melt (—◇—) and intermetallics (—▪—) in the In–La system, according to our optimized thermodynamic model, and data from literature: △ [13], ■ [15], ∗ [6, 20] (similar values), - -○- - [17], - -×- - [2].

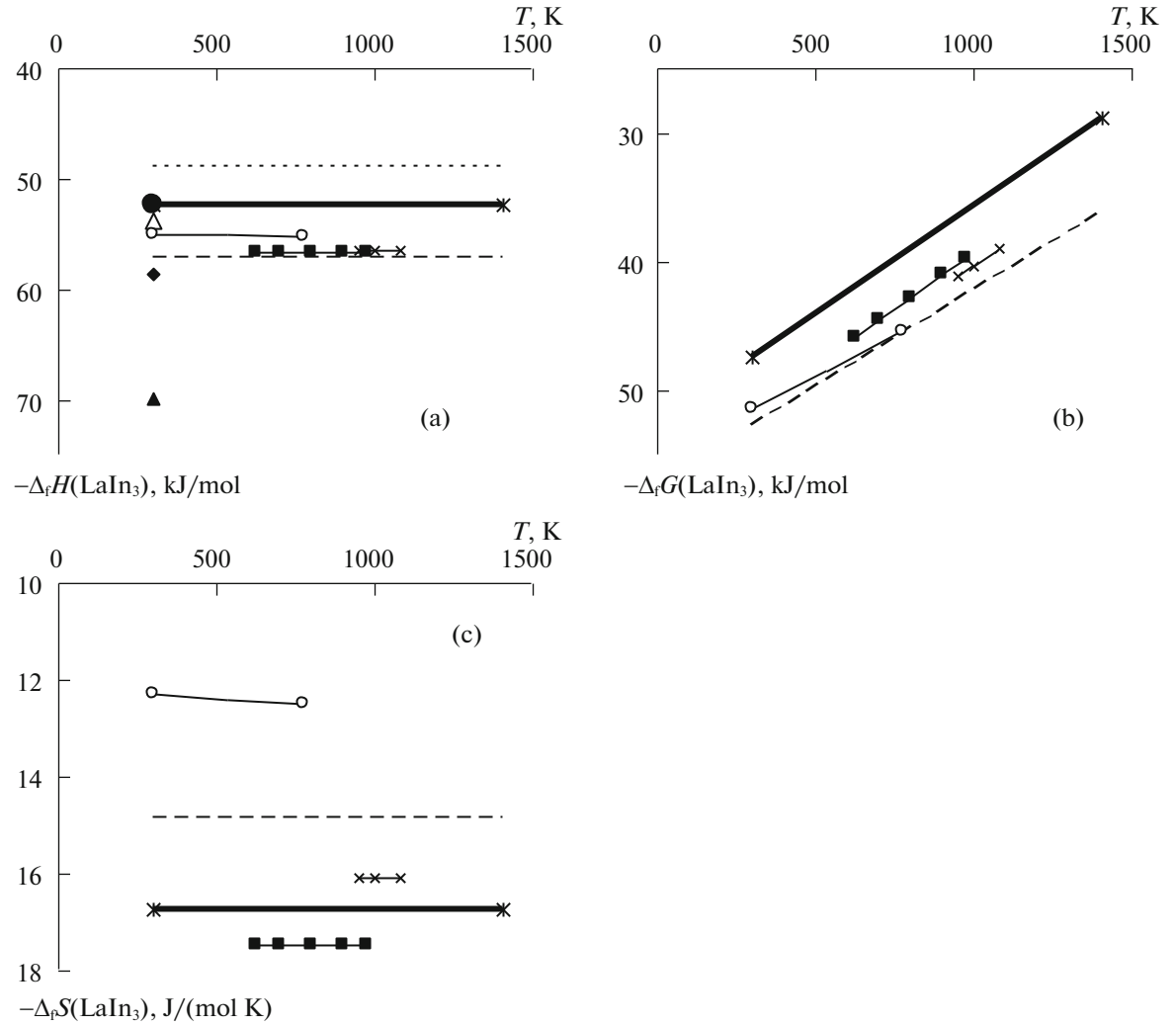

Fig. 7. Enthalpies (a), Gibbs energies (b) and entropies (c) of formation of the $LaIn_3$ intermetallic from the pure solid components, determined using e.m.f. method (—▪— [6], —×— [18]), calorimetry (● [13], ▲ [14], ◆ [15], △ [20]), estimated from the dependence for the Ln–In systems (—◇— [21]), from the Miedema model (- - - - - [17]), CALPHAD method (— — [2]), and optimized by us (—✱—).

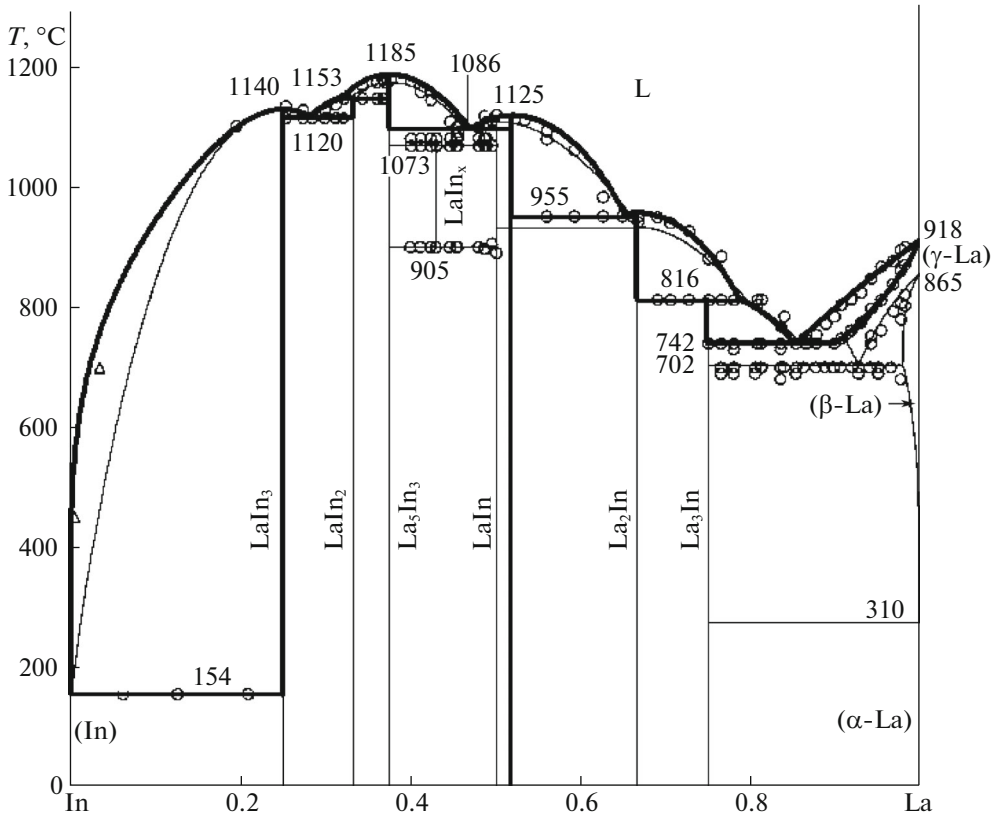

Fig. 8. Modeled phase diagram of the In–La system (liquidus and solidus are bold curves/polylines) compared to the data from literature–experimental (○ [5], △ [6]) and CALPHAD method (—— [2]).

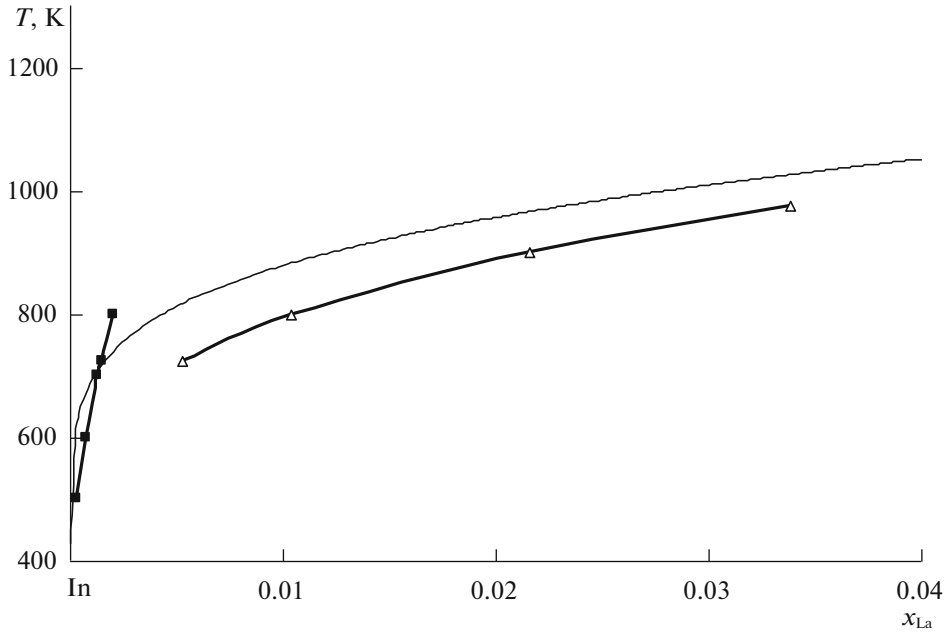

Fig. 9. Liquidus curves (for the melt—$LaIn_3$ equilibrium) for indium-rich alloys, according to our calculation (——); the data [6] (—△—) and [7] (—■—).

reliability has been additionally trusted with the new experimental data.

REFERENCES

1. S. P. Yatsenko, *Indium. Properties and Application* (Nauka, Moscow, 1987) [in Russian].
2. Y. Wei, X. Su, F. Yin, Z. Li, X. Wu, and C. Chen, J. Alloys Compd. **333**, 118 (2002).
3. F. Gao, S. L. Wang, C. P. Wang, and X. J. Liu, CALPHAD: Comput. Coupling Phase Diagrams Thermochem. **35**, 1 (2011).
4. V. V. Berezutskii, M. I. Ivanov, M. A. Shevchenko, and V. S. Sudavtsova, Powder Metall. Metal Ceram. **53**, 693 (2015).
5. O. D. McMasters and K. A. Gschneidner, Jr., J. Less-Common Met. **38**, 137 (1974).
6. V. A. Degtyar', A. P. Bayanov, L. A. Vnuchkova, and V. V. Serebrennikov, Izv. Akad. Nauk SSSR, Met., No. 4, 149 (1971).
7. E. N. Dieva, Tr. Inst. Khim., Ural. Nauch. Tsentr AN SSSR **29**, 98 (1974).
8. V. A. Lebedev, *Thermochemistry of Alloys of Rare-Earth and Actinide Elements, The Handbook,* Ed. by V. A. Lebedev, V. I. Kober, and L. F. Yamshchikov (Metallurgiya, Chelyabinsk, 1989) [in Russian].
9. S. P. Yatsenko, A. A. Semyannikov, H. O. Shakarov, and E. G. Fedorova, J. Less-Common Met. **90**, 95 (1983).
10. S. Delfino, A. Saccone, and R. Ferro, J. Less-Common Met. **102**, 289 (1984).
11. A. Palenzona and S. Cirafici, Bull. Alloy Phase Diagrams **10**, 580 (1989).
12. *Binary Alloy Phase Diagrams,* Ed. by T. B. Masalsky, 2nd ed. (ASM International, Metals Park, OH, 1990).
13. A. Palenzona and C. Cirafici, Thermochim. Acta **9**, 419 (1974).
14. V. A. Novozhenov, T. M. Shkol'nikova, and V. V. Serebrennikov, Zh. Fiz. Khim. **49**, 3012 (1975).
15. A. Borsese, A. Calabreta, S. Delfino, and R. Ferro, J. Less-Common Met. **51**, 45 (1977).
16. A. R. Miedema, F. R. De Boer, and R. Boom, CALPHAD: Comput. Coupling Phase Diagrams Thermochem. **1**, 341 (1977).
17. F. R. de Boer, R. Boom, W. C. M. Mattens, A. R. Miedema, and A. K. Niessen, in *Cohesion and Structure,* Ed. by F. R. de Boer and D. G. Pettifor (North-Holland, Amsterdam, 1988).
18. V. I. Kober, V. A. Dubinin, A. I. Kochkin, et al., Izv. Vyssh. Uchebn. Zaved., Tsvetn. Metall., No. 6, 113 (1983).
19. A. P. Bayanov, Izv. Akad. Nauk SSSR, Neorg. Mater., No. 9, 959 (1973).
20. S. V. Meschel and O. J. Kleppa, J. Alloys Compd. **333**, 91 (2002).
21. V. P. Vassiliev, A. Benaissa, and A. F. Taldrik, J. Alloys Compd. **572**, 118 (2013).
22. M. Ivanov, V. Berezutski, and N. Usenko, J. Mater. Res. **102**, 277 (2011).
23. A. T. Dinsdale, CALPHAD: Comput. Coupling Phase Diagrams Thermochem. **15**, 319 (1991).
24. V. G. Kudin, M. A. Shevchenko, I. V. Mateiko, and V. S. Sudavtsova, Zh. Fiz. Khim. **87**, 364 (2013).
25. M. A. Shevchenko, M. I. Ivanov, V. V. Berezutskii, V. G. Kudin, and V. S. Sudavtsova, Russ. J. Phys. Chem. A **88**, 729 (2014).
26. V. S. Sudavtsova, M. A. Shevchenko, V. V. Berezutskii, M. I. Ivanov, and V. G. Kudin, Russ. J. Phys. Chem. A **88**, 200 (2014).
27. M. A. Shevchenko, V. G. Kudin, and V. S. Sudavtsova, in *Modern Problems of Physical Science of Materials,* Tr. IPM, Vol. 21 (Inst. Prikl. Matem. im. Frantsevicha NANU, Kiev, 2012), p. 67 [in Russian].
28. G. Kaptay, Metall. Mater. Trans. A **43**, 531 (2012).